

УДК 539.171.11, 539.171.115

## DATA ON ELASTIC $(p, n)$ CHARGE EXCHANGE: COMPILATION

*E. A. Stokovsky*

Joint Institute for Nuclear Research, Dubna

Data on differential cross sections for elastic  $p(n, p)n$  charge exchange in the kinetic energy range from 50 MeV up to  $\sim 250$  GeV are compiled. Phenomenological parametrizations of the  $|t|$ -dependence at forward angles as well as the energy dependence of the forward differential cross section  $d\sigma(0)/dt$ , valid in this energy range, are suggested. The data at  $|t| \leq 12m_\pi^2$  demonstrate a surprising universal pattern when the initial energy changes within almost 4 orders in magnitude. This pattern is probably determined by  $\pi$ - and  $\rho$ -meson-like exchange interfering contributions to the reaction amplitude. Surprisingly, at energies between 60 and 75 GeV the interference suddenly changes its type from constructive to destructive one, but the relative strength of the two exchanges remains approximately the same. The old-fashioned «two-exponential» parametrization, inspired by high-energy (above 1 GeV) data, has no deep physical meaning for this reaction.

Составлена сводка данных о дифференциальных сечениях упругой  $p(n, p)n$ -перезарядки в диапазоне кинетических энергий от 50 МэВ до  $\sim 250$  ГэВ. Предложена феноменологическая параметризация  $|t|$ -зависимости (при небольших углах) и энергетической зависимости сечений  $d\sigma(0)/dt$ , применимая внутри этого диапазона. Данные при  $|t| \leq 12m_\pi^2$  демонстрируют удивительно универсальный характер  $|t|$ -зависимости дифференциальных сечений при изменении начальной энергии почти на 4 порядка величины. Эта зависимость, по-видимому, определяется  $\pi$ - и  $\rho$ -мезонными вкладами в амплитуду реакции, которые интерферируют друг с другом. Примечательно, что при энергиях между 60 и 75 ГэВ характер интерференции меняется скачком с конструктивного на деструктивный, хотя относительная «сила»  $\pi$ - и  $\rho$ -подобных вкладов почти не меняется. «Двух-экспонентная» параметризация данных о дифференциальных сечениях, бывшая в прежние годы общеупотребительной для диапазона энергий выше 1 ГэВ, не имеет глубокого физического смысла для рассматриваемой реакции.

### INTRODUCTION

Elastic charge-exchange  $n(p, n)p$  reaction is a surprising example of a rather simple binary reaction which is characterized by a stable universal behaviour at small momentum transfers ( $|t| \lesssim 0.2 \text{ GeV}^2/c^2$ ) from low to high energies. This is not quite well understood theoretically up to now.

On the one hand, one may consider this reaction as a «hard elastic scattering», i. e., backward c. m. elastic scattering of neutron by proton. It is a common belief that such reactions are governed by a short-range interaction. If this were true, at low energies, where  $NN$  interaction can be treated within a potential scattering theory and pion exchange plays an important role, this would have been related with the delta-function part of Yukawa's potential, which represents the short-range interaction [1]. Therefore, one might naively expect that the partial  $S$ -wave must determine angular dependence of the differential cross section (at least at low energies), and thus the latter must be rather isotropic. But experimental data show clearly that it is not the case.

On the other hand, this reaction may be considered as a very peripheral process, the «elastic» small-angle scattering, governed by the charged-pion exchange which transfers the charge from the target (proton) to the projectile (neutron). From such a point of view one may expect that the short-range part of the pion-exchange potential is suppressed and the scattering is dominated by its long-range part, resulting in strong angular dependence of the differential cross section with the «forward peak» even at low energies. This is the experimentally observed case. From this point of view, it may be possible to use data on elastic  $p(n,p)n$  charge exchange for extraction of the pion–nucleon coupling constant from the experimental data, as T. E. O. Ericson suggested in the 1990s.

At rather high energies, where the potential scattering theory is not an adequate framework for data analysis, Regge pole phenomenology has long been used for the data interpretation. But in case of the  $NN$  charge exchange it was in contradiction with the experiment: it predicts dip in the differential cross section at small  $|t|$  instead of the experimentally observed sharp peak. Moreover, with the widely used parametrization of various moderate  $|t|$  cross sections as  $\exp(bt)^1$ , the slope parameter at very small  $|t|$  was unusually big ( $\sim 50 \div 100 \text{ GeV}^{-2}/c^{-2}$ ) and could not be explained easily. Specially invented «explanations» of these facts were suggested (for example, a subtle «conspirations» of Regge trajectories, etc. [3]). An alternative interpretation was based on the picture of peripheral absorption [4] (which actually corresponds to the suppression of the delta-function part of the «field-theoretical» pion potential in the potential scattering theory): it rather naturally explains the sharp «forward peak» in the differential cross sections.

All these problems are well discussed in the literature. The problems related with the *one-pion-exchange* (OPE) potential were considered in the monography [1]. The Regge phenomenology in the  $NN$  charge-exchange case was reviewed in the book [3]. A rather modern view on the problem was presented in the important paper [5], which was focused on theoretical problems mostly. Although it contains a parametrization of the existing data close to the one presented here, the data tables were not presented there<sup>2</sup>.

The goal of the present compilation is twofold. First, it is aimed at presenting a convenient and sufficiently accurate unified parametrization of the known data on differential  $n(p,n)p$  cross sections at small  $|t|$  ( $\lesssim 0.2 \text{ GeV}^2/c^2$ ) in the kinetic energy interval from 50 MeV up to 250 GeV, which can be used for planning new experiments as well as for theoretical analysis of the process. The second aim is to collect in one place the data from different experiments performed since the sixties of the last century, which are scattered in the literature. The publication of the compilation was stimulated by encouraging discussions with V. V. Glagolev and Yu. A. Troyan, to whom the author expresses his deep gratitude.

### PARAMETRIZATION OF THE $n(p,n)p$ DATA

As was mentioned in the Introduction, there are arguments (see, for example, the book [1]) that the OPE contribution to the elastic  $(p,n)$  charge-exchange amplitude must be calculated without the part corresponding to the  $\delta$ -function term in the  $NN$  OPE potential in coordinate

---

<sup>1</sup>This parametrization was introduced for the first time in papers [2] and after those papers became immediately a «self-evident common place» in particle physics.

<sup>2</sup>The first version of this compilation was done independently and before paper [5] was published.

space. This means that partial waves with low orbital momenta  $L$  (in particular, the  $S$ -wave) contribute very little to the reaction amplitude. This corresponds qualitatively to Jackson's «peripheral absorption» of the low- $L$  partial waves for reactions with pion exchange (see, for example, discussion of the problem in Refs. [3,4]).

According to this prescription, one can write the following phenomenological form of the elastic charge-exchange cross section at small  $|t|$  (when the  $t$ - and  $u$ -regions are well separated) in the form which includes both  $\pi$  and  $\rho$  exchanges and their interference:

$$\frac{d\sigma}{dt}(t) = \frac{d\sigma}{dt}(0) \frac{R(t)}{R(0)}, \quad (1)$$

$$R(t) = \frac{f_\pi^2}{(1 + \tau_\pi)^2} + a_\rho^2 \frac{f_\rho^2}{(1 + \tau_\rho)^2} + a_\rho \frac{f_\pi f_\rho}{(1 + \tau_\pi)(1 + \tau_\rho)}, \quad (2)$$

$$\tau_\pi = \frac{|t|}{m_\pi^2}, \quad \tau_\rho = \frac{|t|}{m_\rho^2}, \quad (3)$$

$$f_\pi = (\Lambda_\pi^2 - m_\pi^2)/(\Lambda_\pi^2 - t) = \frac{1.67054}{1.69 + |t|}, \quad (4)$$

$$f_\rho = (\Lambda_\rho^2 - m_\rho^2)/(\Lambda_\rho^2 - t) = \frac{1.3702}{1.96 + |t|}. \quad (5)$$

Here the numerical values (in  $\text{GeV}^2/c^2$ ) of the parameters of the meson-baryon vertex form factors  $f_\pi$  and  $f_\rho$  in Eqs. (4) and (5) are taken from Ref. [7]. Two free parameters  $a_\rho$  (which determines a relative strength of the contribution from  $\rho$  exchange) and  $d\sigma(0)/dt$  must be found from the best fit of the data. This parametrization will be called here a  $(\pi + \rho)$ -motivated parametrization.

It can easily be seen from Eqs.(1) and (2) that, at small  $\tau_\pi (\ll 1)$  in a limited region where the  $\pi$ -like contribution in Eq.(2) dominates, one may indeed use the old-fashioned exponential parametrization:

$$\begin{aligned} \frac{d\sigma}{dt}(t) &= \frac{d\sigma}{dt}(0) e^{Bt}, \\ B &= \frac{2f_\pi^2 + a_\rho f_\rho f_\pi}{R(0)} \frac{1}{m_\pi^2}, \\ R(0) &= f_\pi^2 + a_\rho f_\rho f_\pi + a_\rho^2 f_\rho^2 \end{aligned} \quad (6)$$

with the slope parameter  $B$  of order of  $1/m_\pi^2 \sim 45 \text{ GeV}^{-2}/c^{-2}$ . At higher 4-momentum transfers, where still  $\tau_\rho \ll 1$  but  $\tau_\pi \gg 1$  already ( $\rho$ -like term dominates), the slope parameter will be much smaller, of order of  $1.4 \cdot 1/m_\rho^2 \sim 2.4 \text{ GeV}^{-2}/c^{-2}$ , while in the intermediate region (both terms are of the same strength) it will be of order of  $B \sim 1/m_\rho \cdot 1/m_\pi \sim 9 \text{ GeV}^{-2}/c^{-2}$ . So, the slope parameter  $B$  is dependent upon  $t$  and has almost no physical meaning.

Initially, only the data tabulated in the refereed journals were used in the compilation. For the present version, a bulk of data was added from the SAID data base; low-energy data were also added from the Nijmegen data base. Access to both data bases was possible via their WWW pages [6]. The selection of the data is commented in the Appendix.

Not all the data on differential cross sections are accurate enough to allow reasonable two-parameter fit. Therefore the analysis was performed in two steps. As can be seen

from Eqs. (1) and (2), when the parameter  $a_\rho$  is fixed, the angular dependence pattern of the differential cross sections is completely determined, which makes it possible to find the forward differential cross section  $d\sigma(0)/dt$  even for data with poor accuracy on  $d\sigma/dt$ . Therefore, at the first step, the free parameter  $a_\rho$  of the function  $R(t)$  defined in Eq. (2) was found by using a subset of the available data (a *basic subset*), and its energy dependence was inspected. After determining the  $a_\rho$ , an averaged value of this parameter was found and fixed. In this way the law of extrapolation to the  $|t| = 0$  point was fixed.

**Table 1. Results of the  $(\pi + \rho)$ -motivated fit (two parameters) in the region  $0 < t \leq |t|_{\max}$  at low energies ( $t$ -dependent systematic errors are ignored)**

Reference	$p_{\text{lab}}, \text{ GeV}/c$	$a_\rho$	$\chi^2/\text{DoF}$	$ t _{\max}, \text{ GeV}^2/c^2$
Roenquist [26]	0.435	$1.417 \pm 0.021$	3.5	0.05
Measday [17]	0.509	$1.398 \pm 0.055$	2.1	0.16
«Uppsala» [16]	0.635	$1.236 \pm 0.016$	4.7	0.08
Bonner [8]	0.575	$1.463 \pm 0.032$	2.0	$\sim 0.07$
	0.635	$1.411 \pm 0.028$	2.3	0.09
	0.725	$1.571 \pm 0.031$	1.8	0.12
	0.845	$1.404 \pm 0.590$	0.1	0.16
	1.115	$1.341 \pm 0.011$	8.9	0.12
	1.175	$1.326 \pm 0.013$	8.1	0.12
Bizard [9]	1.133	$1.424 \pm 0.025$	3.6	0.12
Keeler [10]	0.838	$1.624 \pm 0.017$	8.3	0.13
	0.980	$1.636 \pm 0.024$	6.1	0.13
Northcliff [13]	1.036	$1.502 \pm 0.761$	0.1	0.12
Shepard [24, 25]	0.612	$1.397 \pm 0.040$	1.4	0.15
	0.637	$1.314 \pm 0.034$	2.8	0.15
	0.662	$1.274 \pm 0.032$	2.7	0.15
	0.687	$1.225 \pm 0.031$	3.6	0.15
	0.712	$1.275 \pm 0.034$	1.4	0.15
	0.741	$1.280 \pm 0.033$	3.8	0.15
	0.784	$1.167 \pm 0.025$	4.1	0.15
	0.829	$1.311 \pm 0.040$	5.1	0.15
	0.874	$1.195 \pm 0.029$	3.8	0.25
	0.923	$1.373 \pm 0.052$	3.0	0.25
	0.974	$1.121 \pm 0.031$	4.3	0.25
	1.045	$1.381 \pm 0.054$	3.2	0.25
	1.145	$1.176 \pm 0.055$	2.3	0.25
	1.281	$1.043 \pm 0.020$	1.8	0.15
	1.484	$1.097 \pm 0.048$	1.5	0.15
1.730	$1.039 \pm 0.042$	3.3	0.15	

At the second step, the fit was repeated for all the data, the  $d\sigma(0)/dt$  values were found, and the energy dependence of the forward differential cross section was investigated.

**Fixing the Angular Dependence Pattern.** Results of the two-parameter fit are presented in Tables 1 and 2. The value of  $a_\rho$  is almost independent of the initial momentum up to 60 GeV/c:

$$a_\rho = 1.335 \pm 0.051. \quad (7)$$

Without data of Ref. [24] the averaged value was

$$a_\rho = 1.394 \pm 0.059, \quad (8)$$

which differs from the value given above within the error bars but matches the value obtained for high energies not so well. Finally, the value  $a_\rho = 1.335 \pm 0.051$  at  $p_{\text{lab}} \leq 60$  GeV was chosen and kept as fixed for further analysis.

At higher momenta the  $a_\rho$  suddenly changes its sign but remains almost constant again (see Figs. 1 and 2):

$$a_\rho = -1.168 \pm 0.042; \quad \chi^2 = 0.8/(6 \text{ points}). \quad (9)$$

**Table 2. Results of the ( $\pi + \rho$ )-motivated fit (two parameters) in the region  $0 < t \leq |t|_{\text{max}}$  at high energies ( $t$ -dependent systematic errors are ignored)**

Reference	$p_{\text{lab}}$ , GeV/c	$a_\rho$	$\chi^2/\text{DoF}$	$ t _{\text{max}}$ , GeV/c
Manning [30]	8	$1.124 \pm 0.096$	1.1	0.15
Boemer [33]	10.5	$1.251 \pm 0.045$	2.5	0.20
	13.5	$1.276 \pm 0.052$	1.6	0.20
	16.5	$1.224 \pm 0.058$	1.8	0.20
	18.5	$1.150 \pm 0.048$	1.5	0.20
	20.5	$1.265 \pm 0.048$	1.4	0.20
	22.5	$1.273 \pm 0.065$	1.8	0.20
Babaev [35]	23.5	$1.292 \pm 0.130$	4.9	0.25
	27.5	$1.170 \pm 0.100$	3.1	0.25
	32.5	$0.981 \pm 0.076$	2.4	0.25
	37.5	$1.228 \pm 0.100$	1.4	0.25
	42.5	$1.256 \pm 0.100$	2.2	0.25
	47.5	$1.212 \pm 0.100$	4.5	0.25
	52.5	$1.270 \pm 0.082$	3.3	0.25
	57.5	$1.382 \pm 0.086$	4.7	0.25
62.5	$1.534 \pm 0.110$	3.4	0.25	
Barton [36]	75	$-1.176 \pm 0.092$	1.1	0.20
	105	$-1.365 \pm 0.180$	1.0	0.20
	140	$-1.169 \pm 0.081$	1.1	0.20
	180	$-1.106 \pm 0.065$	0.8	0.20
	220	$-1.157 \pm 0.078$	1.6	0.20
	260	$-1.415 \pm 0.180$	0.7	0.20

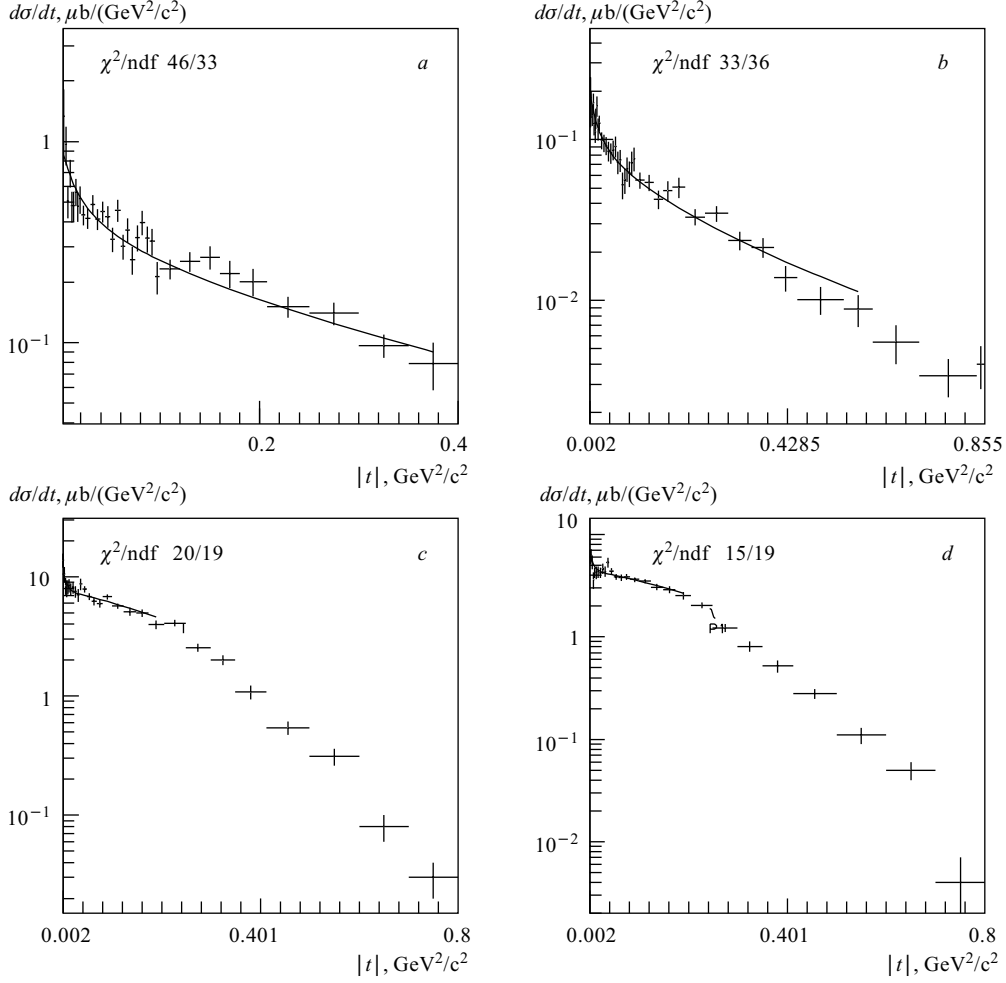


Fig. 1. The  $|t|$ -dependence of the elastic  $p(n,p)n$  charge-exchange differential cross sections below 70 GeV/c (data from Kreisler et al. [34] for 9 GeV/c (a) and 21 GeV/c (b)) and above (data from Barton et al. [36] for 140 GeV/c (c) and 260 GeV/c (d)). Sudden change of the pattern at  $|t| \leq 0.4 \text{ GeV}^2/c^2$  is evident. It corresponds to change in sign of the  $a_\rho$  parameter

The universal pattern of the differential cross sections is demonstrated in Figs. 3–8, where a small sample of data in the interval of incident energies from 50 MeV to 70 GeV is presented. Data at low energies (less than 100 MeV) are shown for illustrative purposes only, because in this region one can calculate these cross sections with a rather high accuracy by using Partial Wave Analysis Interactive Tools (see Refs. [6]). Nevertheless, the suggested approximation works with reasonable accuracy even in this region of very low energies.

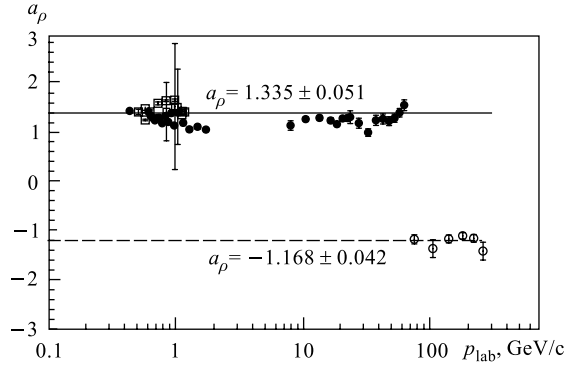


Fig. 2. Momentum dependence of the  $a_\rho$  parameter which determines the relative strength of the  $\rho$  exchange in the total amplitude of the elastic  $p(n, p)n$  charge exchange. Lines: fitted average as explained in text

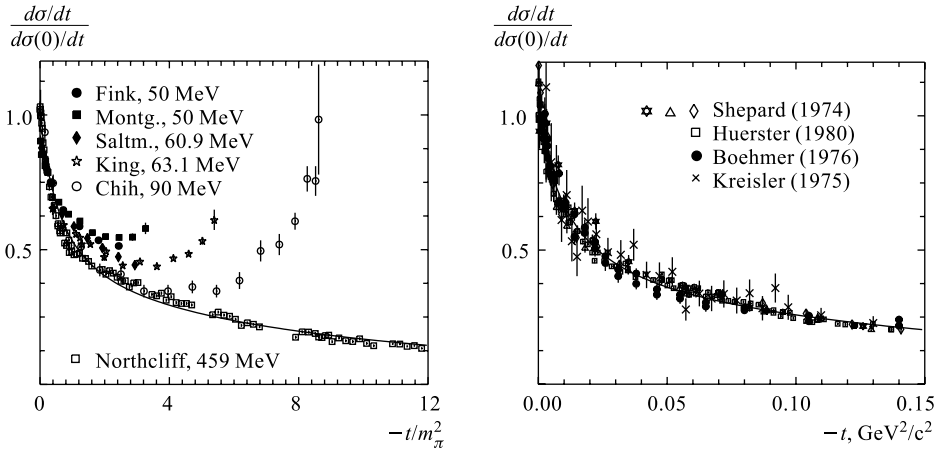


Fig. 3. The universal pattern of the  $d\sigma/dt$  (solid line) versus the dimensionless ratio  $|t|/m_\pi^2$ . The apparent forward-backward symmetry seen in the data around  $T_{\text{lab}} \sim 50$  MeV is accidental

Fig. 4. The universal pattern of the  $d\sigma/dt$  (solid line) and a sample of high-energy data together with the low-energy one

**Energy Dependence of  $d\sigma(0)/dt$ .** Full set of data on forward differential cross sections of elastic  $p(n, p)n$  charge exchange obtained in our analysis is presented in Tables 3 and 4. Some data on  $d\sigma(0)/dt$  were published in original papers without presenting the corresponding differential cross sections. Therefore, the present analysis could not be made for those data; we include these values in Tables 3 and 4 as they were published. The values of  $d\sigma(0)/dt$  at  $p_{\text{lab}} \geq 75$  GeV/c are given from our fit of data from Ref. [36] with *fixed*  $a_\rho = -1.168$ . Data from Ref. [23] are excluded from Table 3 because those are now obsolete.

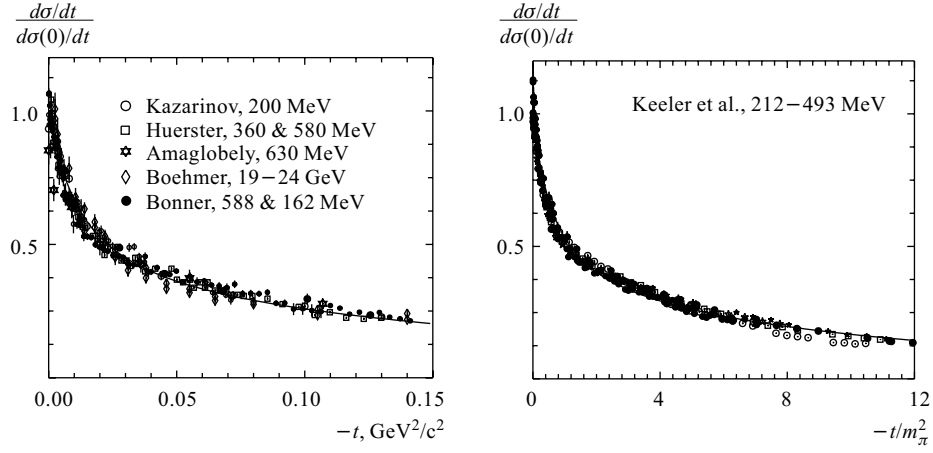


Fig. 5. The universal pattern of the  $d\sigma/dt$  (solid line) and a sample of high-energy data together with the low-energy one. Rather high quality of the old data from LNP of JINR is evident

Fig. 6. The universal pattern of the  $d\sigma/dt$  (solid line) versus the dimensionless ratio  $|t|/m_\pi^2$

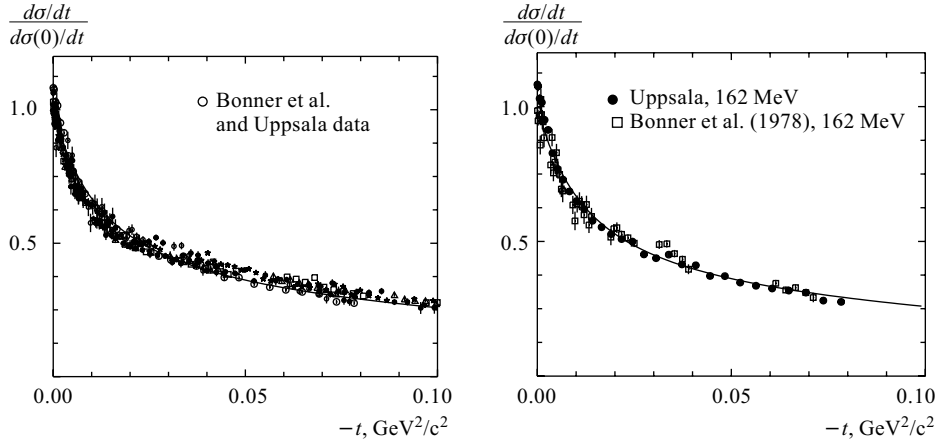


Fig. 7. The universal pattern of the  $d\sigma/dt$  (solid line) and a sample of low-energy data

Fig. 8. The universal pattern of the  $d\sigma/dt$  (solid line) versus  $t$ . Data at 162 MeV from Refs. [8, 16] are compared

The dependence of  $d\sigma(0)/dt$  on the initial momentum is satisfactorily described by an empirical formula

$$\frac{d\sigma}{dt}(0) = \frac{A}{(p_{\text{lab}}/m_n)^{\gamma(p_{\text{lab}}/m_n)}}, \quad \gamma = n - c \ln(p_{\text{lab}}/m_n), \quad (10)$$

Table 3. Compilation of data on  $d\sigma(0)/dt$  for elastic  $p(n, p)n$  charge exchange at low energies ( $(\pi + \rho)$ -motivated fit). Both statistical and systematic (as given in the cited papers) errors are presented

$T_n$ , MeV	$p_{\text{lab}}$ , MeV/c	$d\sigma(0)/dt$ , mb/(GeV <sup>2</sup> /c <sup>2</sup> )	$T_n$ , MeV	$p_{\text{lab}}$ , MeV/c	$d\sigma(0)/dt$ , mb/(GeV <sup>2</sup> /c <sup>2</sup> )
50	311	2872 ± 18 ± ? [18]	344.3	875	212 ± 0.64 ± 16 [8]
50	311	2841 ± 13 ± ? [20]	350	883	222 ± 0.92 ± 11 [14]
60.9	344	1793 ± 17 ± ? [21]	350	883	210 ± 1.1 ± 11 [14]
63.1	350	1913 ± 10 ± ? [22]	365	905	190 ± 0.65 ± 14 [8]
90	421	946 ± 14 ± ? [19]	378	923	175 ± 2.0 ± 22 [24]
96	435	998 ± 2.6 ± 41 [26]	386	935	176 ± 0.60 ± 13 [8]
108	464	854 ± 20 ± 26 [15]	407.3	965	165 ± 0.42 ± 12 [8]
128	507	657 ± 7.6 ± 46 [12]	414	974	158 ± 1.7 ± 19 [24]
129	509	650 ± 6.3 ± 42 [17]	418	980	171 ± 0.60 ± 5.6 [10]
129	509	670 ± 4.3 ± 47 [11]	418	980	171 ± 0.64 ± 5.6 [10]
150	552	527 ± 3.9 ± 34 [17]	421.4	985	164 ± 27 ± 8.2 [9]
162	575	533 ± 1.5 ± ? [16]	428.9	995	165 ± 0.42 ± 12 [8]
162	575	482 ± 2.5 ± 35 [8]	450.9	1025	148 ± 0.44 ± 11 [8]
177.9	605	435 ± 2.3 ± 32 [8]	457.2	1033	146 ± 0.72 ± 7.3 [9]
182	612	325 ± 3.0 ± 41 [24]	459.3	1036	137 ± 0.32 ± 9.6 [13]
194.5	635	393 ± 2.1 ± 30 [8]	466	1045	138 ± 1.6 ± 36 [24]
196	637	322 ± 2.8 ± 45 [24]	473.2	1055	138 ± 0.39 ± 10 [8]
200	645	413 ± 2.6 ± 83 [27]	493	1081	142 ± 0.66 ± 6.0 [10]
200	645	398 ± 3.3 ± 80 [27]	494.6	1084	122 ± 19 ± 6.1 [9]
210	662	313 ± 2.7 ± 40 [24]	495.7	1085	130 ± 0.29 ± 10 [8]
211.5	665	360 ± 1.9 ± 27 [8]	518.5	1115	123 ± 0.26 ± 9.2 [8]
212	666	381 ± 0.63 ± 12 [10]	532	1132	118 ± 0.49 ± 5.9 [9]
224	687	285 ± 2.6 ± 35 [24]	541.6	1145	116 ± 0.27 ± 8.7 [8]
229.1	695	330 ± 1.7 ± 25 [8]	542	1145	99.9 ± 1.5 ± 11 [24]
239	712	268 ± 2.4 ± 33 [24]	564.9	1175	109 ± 0.27 ± 8.2 [8]
247.2	725	305 ± 1.6 ± 23 [8]	570.9	1183	100 ± 0.37 ± 5.0 [9]
257	741	244 ± 2.1 ± 31 [24]	588.4	1205	101 ± 0.30 ± 7.6 [8]
265.8	756	284 ± 0.89 ± 21 [8]	630	1257	99.8 ± 3.0 ± 20 [28]
284	784	198 ± 1.5 ± 26 [24]	649	1281	65.1 ± 1.0 ± 7 [24]
284.8	785	252 ± 0.85 ± 19 [8]	747	1400	62 ± 6 (tot.) [29]
304.2	815	248 ± 0.76 ± 19 [8]	817	1484	52.7 ± 0.78 ± 6.3 [24]
313	829	200 ± 2.0 ± 27 [24]	1028	1729	39.9 ± 0.57 ± 4.3 [24]
319.2	838	239 ± 0.54 ± 9.3 [10]	1592	2350	20 ± 6 (tot.) [29]
324.1	845	213 ± 25 ± 16 [8]	2205	3000	11 ± 2 (tot.) [29]
344	874	177 ± 1.5 ± 21 [24]	2734	3550	7.1 ± 1 (tot.) [29]

where the parameters are as follows:

$$A = (166.1 \pm 1.8) \text{ mb}/(\text{GeV}^2/c^2), \quad n = 2.432 \pm 0.008, \quad c = 0.1031 \pm 0.0032. \quad (11)$$

**Table 4. Compilation of data on  $d\sigma(0)/dt$  for elastic  $p(n,p)n$  charge exchange at high energies (( $\pi + \rho$ )-motivated fit). Both statistical and systematic (as given in the cited papers) errors are presented**

$T_n$ , GeV	$p_{lab}$ , GeV/c	$d\sigma(0)/dt$ , $\mu\text{b}/(\text{GeV}^2/c^2)$	$T_n$ , GeV	$p_{lab}$ , GeV/c	$d\sigma(0)/dt$ , $\mu\text{b}/(\text{GeV}^2/c^2)$
<i>7.116</i>	8	<i><math>788 \pm 21 \pm 225</math></i> [30]	23.08	24.0	$215 \pm 3.6 \pm 64$ [31]
7.116	8	$1658 \pm 2.4 \pm 526$ [31]	24.08	25.0	$172 \pm 3.8 \pm 14$ [34]
8.908	9.8	$993 \pm 24 \pm 153$ [34]	26.38	27.3	$147 \pm 3.5 \pm 13$ [34]
9.604	10.5	$723 \pm 7.1 \pm 136$ [33]	26.58	27.5	$134 \pm 3.3 \pm 21$ [35]
11.70	12.6	$511 \pm 10 \pm 55$ [34]	31.58	32.5	$95.2 \pm 2.3 \pm 13$ [35]
12.59	13.5	$461 \pm 4.8 \pm 72$ [33]	36.57	37.5	$82.7 \pm 1.7 \pm 11$ [35]
14.09	15.0	$363 \pm 9.8 \pm 33$ [34]	41.57	42.5	$71.7 \pm 2.0 \pm 8.8$ [35]
15.59	16.5	$338 \pm 4.2 \pm 43$ [33]	46.57	47.5	$56.6 \pm 1.2 \pm 6.6$ [35]
16.09	17.0	$310 \pm 8.1 \pm 26$ [34]	51.57	52.5	$52.3 \pm 1.0 \pm 6.8$ [35]
17.59	18.5	$286 \pm 3.3 \pm 38$ [33]	56.57	57.5	$47.5 \pm 0.8 \pm 6.1$ [35]
18.08	19.0	$250 \pm 6.3 \pm 20$ [34]	61.57	62.5	$45.7 \pm 0.8 \pm 6.5$ [35]
18.28	19.2	$261 \pm 3.2 \pm 82$ [31]	74.07	75.0	$27.6 \pm 1.5 \pm 4$ [36]
19.58	20.5	$243 \pm 2.6 \pm 34$ [33]	104.1	105	$19.6 \pm 1.1 \pm 3$ [36]
20.08	21.0	$222 \pm 5.4 \pm 17$ [34]	139.1	140	$15.3 \pm 0.7 \pm 2.3$ [36]
21.58	22.5	$204 \pm 2.7 \pm 26$ [33]	179.1	180	$11.7 \pm 0.5 \pm 1.8$ [36]
22.08	23.0	$192 \pm 4.3 \pm 15$ [34]	219.1	220	$9.2 \pm 0.4 \pm 1.4$ [36]
22.58	23.5	$190 \pm 5.3 \pm 36$ [35]	259.1	260	$8.00 \pm 0.4 \pm 1.2$ [36]

These parameters were determined on 82 data points from those given in Tables 3 and 4; the italicized points were not included in this fit. The quality of the fit is acceptable as one can see from Fig. 9 (average  $\chi^2 = 4.1$  per data point). To see details of the energy dependence for the data measured in various experiments, in Fig. 9, *a, b* the interval from 300 MeV to 10 GeV is shown; Fig. 9, *c* shows the data on  $d\sigma(0)/dt$  in the full energy interval explored.

Performing this fit, we have taken into account both statistical and systematic errors from Tables 3 and 4. For some data the estimation of the systematic uncertainty was not possible; these cases are indicated in Tables 3 and 4 by the question mark.

## APPENDIX

**Comments on the Intermediate-Energy Data.** Being obsolete now, *the data of Ref. [23]* were excluded from any fits. They were taken from figures for two values of the beam energy: 580 and 360 MeV.

*The data from Ref. [24]* were obtained at 12 energies from  $T_n = 182$  MeV to  $T_n = 1028$  MeV, and tabulated. They were used only for determination of the  $a_\rho$  parameter, which can be justified by Figs. 7 and 8, but they were completely excluded from the fit of the *energy dependence* of the  $d\sigma(0)/dt$ , because of the apparent energy-dependent systematic errors (see Fig. 9, *a*). The systematic normalization error given in paper [24] is as large as 25%; we assumed it to be  $\pm 12.5\%$ .

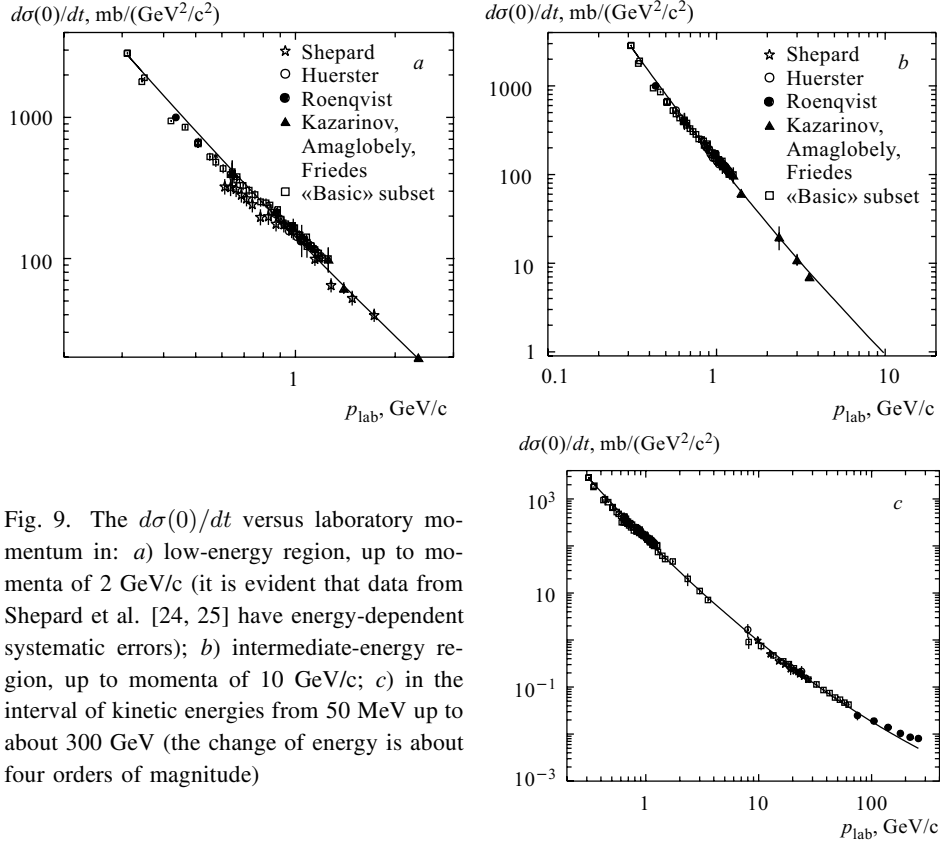


Fig. 9. The  $d\sigma(0)/dt$  versus laboratory momentum in: *a*) low-energy region, up to momenta of 2 GeV/c (it is evident that data from Shepard et al. [24, 25] have energy-dependent systematic errors); *b*) intermediate-energy region, up to momenta of 10 GeV/c; *c*) in the interval of kinetic energies from 50 MeV up to about 300 GeV (the change of energy is about four orders of magnitude)

Both sets are still presented in the data tables for completeness and for illustration of their quality.

The data from Ref. [26] were obtained at  $T_n = 96$  MeV; the absolute normalization accuracy quoted in paper [26] is  $\pm 4\%$ .

The data from Ref. [29] were presented only in graphs with arbitrary units for the ordinate axis; therefore, the values originally found by the authors are included in Table 3.

**Comments on the Data in the High-Energy Region.** In general, the statistical accuracy of these data is worse than what is typical for intermediate-energy experiments.

The data from Ref. [30] are probably biased: the value  $d\sigma(0)/dt = (0.852 \pm 0.022 \pm 0.26)$  mb/(GeV/c)<sup>2</sup> with fit in the interval  $|t| \leq 0.12$  GeV<sup>2</sup>/c<sup>2</sup> is lower than expected.

The data from Ref. [32] on differential cross sections at incident momenta from 3 to 12 GeV/c were presented only in figures; the quality of the figures did not allow inclusion of these data in the analysis.

The data from Ref. [33] were obtained at neutron momenta from 9 up to 23 GeV/c; this interval was divided into six parts, and for each of them the differential cross sections were tabulated. The normalization errors were momentum-dependent and varied from 5 to 12% at lowest energy of this experiment. The central value of the incident momentum is given

in Tables 3 and 4 for these data. Fit of these data and data from Ref. [34] was made by the «standard» function in the region  $|t| \leq 0.15 \text{ GeV}^2/c^2$ .

The data from Ref. [35] were obtained at neutron momenta from 23.5 up to 62.5 GeV/c; for each energy the differential cross sections were tabulated. The normalization errors were momentum-dependent and varied from 3 % at momenta above 42.5 GeV/c to 12 % at lowest energy of this experiment.

These data as well as the data from Refs. [36, 37] must be used with precautions. The initial energies of those experiments are above threshold for diffraction production of charmed particles (not discovered at the time when the discussed experiments were performed). One may assume, from the published descriptions of the experiments, that such processes might be not completely suppressed and could produce a background, which means that the claimed information about *genuine elastic* ( $n, p$ ) charge exchange might be spoiled by such a background. Unfortunately, after discovery of the charmed particles there were no more experiments on the elastic ( $n, p$ ) charge exchange at high energies, and the data from the experiments [35–37] remain unique.

#### REFERENCES

1. *Ericson T. E. O., Weise W.* Pions and Nuclei. Oxford: Clarendon Press, 1988.
2. *Belenky S.* // Pis'ma ZhETF. 1956. V. 30. P. 983;  
*Grishin V. G., Saitov I. S.* // Pis'ma ZhETF. 1957. V. 33. P. 105 (references are given according to the Russian edition).
3. *Collins P. D. B., Squires E. J.* Regge Poles in Particle Physics // Springer Tracts in Modern Physics. Berlin; Heidelberg; N. Y.: Springer-Verlag, 1968. V. 45; translated into Russian by A. I. Naumov / Ed. A. M. Brodsky. M.: Mir, 1971.
4. *Jackson J. D.* // Rev. Mod. Phys. 1965. V. 37. P. 484.
5. *Gibbs W. R., Loiseau B.* // Phys. Rev. C. 1994. V. 50. P. 2742.
6. Data tables are taken in part from WWW URL addresses:  
<http://gwdac.phys.gwu.edu/> ([http://gwdac.phys.gwu.edu/analysis/nn\\_analysis.html](http://gwdac.phys.gwu.edu/analysis/nn_analysis.html) for SAID data base) and <http://nn-online.sci.kun.nl/> (<http://nn-online.sci.kun.nl/NN/nnsearch.html> for Nijmegen University data base).
7. *Oset E., Shiino E., Toki H.* // Phys. Lett. B. 1989. V. 224. P. 249.
8. *Bonner B. E. et al.* // Phys. Rev. Lett. 1978. V. 41. P. 1200.
9. *Bizard G. et al.* // Phys. Rev. Lett. 1976. V. 36. P. 497; Phys. Rev. D. 1977. V. 15. P. 36.
10. *Keeler R. K. et al.* // Nucl. Phys. A. 1982. V. 377. P. 529.
11. *Howard V. J. et al.* // Nucl. Phys. A. 1974. V. 218. P. 140.
12. *Hobbie R. K., Miller D.* // Phys. Rev. 1960. V. 120. P. 2201.
13. *Northcliff L. C. et al.* // Phys. Rev. C. 1993. V. 47. P. 36.

14. *Ashmore A. A. et al.* // Nucl. Phys. 1962. V. 36. P. 258.
15. *Scanlon J. P. et al.* // Nucl. Phys. 1963. V. 41. P. 401.
16. *Ericson T. E. O. et al.* // Phys. Rev. Lett. 1995. V. 75. P. 1046.
17. *Measday D. F.* // Phys. Rev. 1966. V. 142. P. 584.
18. *Fink G. et al.* // Nucl. Phys. A. 1990. V. 518. P. 561.
19. *Chih C. Y. et al.* // Phys. Rev. 1957. V. 106. P. 539.
20. *Montgomery T. C. et al.* // Phys. Rev. C. 1977. V. 16. P. 499.
21. *Saltmarsh M. J. et al.* (1971), data can be found in the paper of *Arndt R. A. et al.* // Phys. Rev. D. 1973. V. 8. P. 1397.
22. *King N. S. P. et al.* // Phys. Rev. C. 1980. V. 21. P. 1185.
23. *Huerster W. et al.* // Phys. Lett. B. 1980. V. 90. P. 367.
24. *Shepard P. F. et al.* // Phys. Rev. D. 1974. V. 10. P. 2735; see also their first results in Ref. [25].
25. *Mischke R. E., Shepard P. F., Devlin T. J.* // Phys. Rev. Lett. 1969. V. 23. P. 542.
26. *Roenquist T. et al.* // Phys. Rev. C. 1992. V. 45. P. R496.
27. *Kazarinov Yu. M., Simonov Yu. N.* // ZhETF. 1962. V. 43. P. 35; data tables are in: *Benary O. et al. NN and ND Interactions (above 0.5 GeV/c) — A Compilation. UCRL-20000 NN, LRL. Berkeley, 1970.*
28. *Amaglobely N. S., Kazarinov Yu. M.* // ZhETF. 1959. V. 37. P. 1518; see tables in: *Benary O. et al. NN and ND Interactions (above 0.5 GeV/c) — A Compilation. UCRL-20000 NN, LRL. Berkeley, 1970.*
29. *Friedes J. L. et al.* // Phys. Rev. Lett. 1964. V. 15. P. 38; the data are taken from figures.
30. *Manning G. et al.* // Nuovo Cim. 1966. V. 41. P. 167.
31. *Engler J. et al.* // Phys. Lett. B. 1971. V. 34. P. 528.
32. *Miller E. L. et al.* // Phys. Rev. Lett. 1971. V. 26. P. 984.
33. *Boehmer V. et al.* // Nucl. Phys. B. 1976. V. 110. P. 205.
34. *Kreisler M. N. et al.* // Nucl. Phys. B. 1975. V. 84. P. 3.
35. *Babaev A. et al.* // Nucl. Phys. B. 1976. V. 110. P. 189.
36. *Barton H. R., Jr., et al.* // Phys. Rev. Lett. 1976. V. 37. P. 1656.
37. *Barton H. R., Jr., et al.* // Ibid. P. 1659.

Received on July 9, 2003.